PHOTON CORRELATION SPECTROSCOPY AND LIGHT SCATTERING OF EYE LENS PROTEINS AT HIGH CONCENTRATIONS

CHRISTIANE ANDRIES AND JULIUS CLAUWAERT
Department of Biochemistry, Universitaire Instelling Antwerpen, B-2610 Antwerpen, Belgium

ABSTRACT The bovine eye lens protein, α_L crystallin, has been studied with photon correlation spectroscopy and statical light scattering in the concentration range up to 200 g/l in different solvent conditions. At higher concentration ($c > 70$ g/l) the scattering behavior is quite complicated, which results in nonexponential correlation functions. Three methods have been used for the analysis of these correlation functions, namely, cumulantanalysis, sum of two exponentials analysis, and exponential sampling method. These methods resulted in very similar results. The highly concentrated solutions contain two scattering entities: the single α_L crystallin and a rather heterogeneous population of large clusters. The statical light-scattering experiments can be interpreted in the same way and gave consistent results for the dimensions of the large scattering units. The formation of these clusters, which are strong light scatterers, is superimposed on an increasing degree of correlation between the bulk of the α_L-crystallins, resulting in a net decrease of light scattering as a function of concentration.

INTRODUCTION

The cytoplasma of the mammalian eye lens fiber cells consists of ~40% of proteins, which on the basis of their molecular weight and peptide composition can be divided in three classes: α-, β-, and γ-crystallins (Bloemendal, 1982). If all these proteins acted as independent scatterers, then the system would be opaque. Nevertheless, it is not necessary to assume a crystalline or paracrystalline state to explain the observed transparency. Benedek proved that a limited degree of local short-range order is sufficient to explain the transparency (Benedek, 1971).

The increase in light scattering in older and cataractous lenses can be attributed to the formation of larger particles, whose dimensions are comparable to the wavelength of the light. The presence of these larger scattering units has been concluded from biochemical studies (Spector et al., 1971; Stauffer et al., 1974; Siezen et al., 1979). The light-scattering properties of complete lenses have been extensively studied (Tanaka and Benedek, 1975; Jedziniak et al., 1978; Bettelheim and Bettelheim, 1978; Bettelheim and Paunovic, 1979; Bettelheim, 1975, 1978) but very little is known about the specific role of each type of crystallin in maintaining a transparent lens.

The study of homogenous solutions in well-defined solvent conditions will allow more quantitative conclusions in this matter; α_L-crystallin has been chosen because of its higher molecular weight and its concentration in the cytoplasma. This crystallin is highly soluble (up to 250 mg/ml) and it is also believed that physicochemical changes of this protein are important in senile cataract formation (Harding and Dilley, 1976). The use of visible light-scattering techniques is intrinsically relevant for the study of transparency. The use of light scattering and photon correlation spectroscopy under identical conditions gives similar and complementary information. Photon and fluorescence correlation spectroscopy and light scattering of α_L-crystallin up to a volume fraction of 2.5×10^{-2} have taught us that the interaction potential between the proteins at moderate ionic strength ($I = 0.08$) and higher ionic strength ($I = 0.32$) can be described by an extended hard-sphere potential or a shielded coulomb potential (Andries et al., 1983).

Here we studied α_L-crystallin solutions with a protein volume fraction >0.035. Drastic changes occur in the α_L-crystallin solution in this concentration region. The scattered intensity per concentration unit further decreases with increasing concentration and strong forward scattering is observed. The photon correlation function reflects different decay modes: the diffusion of the single α_L-crystallins and of larger units. Both techniques suggest the reversible formation of larger clusters; the formation of these clusters is concentration dependent, but is also influenced by the changes in the interaction between the α_L-crystallins as shown by a change in ionic strength of the solvent or a change in the charge of the α_L-crystallins, which is shown by the study of α_L-crystallins from calf and bovine lenses.

Address all correspondence to Julius Clauwaert.

THEORY

The interactions between macromolecules in solutions induce static and dynamic correlations that can be measured by static and dynamic light scattering. The Einstein-Debye-Zernicke-Prins theory gives the following expression for the Raleigh ratio

$$R_\theta = \kappa \cdot c \cdot M_r \cdot S(\bar{\mathbf{K}}) \cdot P(\bar{\mathbf{K}}) \tag{1}$$

with

$$\kappa = \frac{2\pi^2 n^2}{N_A \lambda^4} \cdot \left(\frac{\delta n}{\delta c}\right)^2,$$

where n is the refractive index, $(\delta n/\delta c)$ is the refractive index increment, λ equals the wavelength of the light, c equals the concentration in grams per liter, M_r equals the molar mass in grams per mole, $S(\bar{\mathbf{K}})$ equals the static structure factor accounting for intermolecular structure, with $\bar{\mathbf{K}}$ equal to the scattering vector $|\bar{\mathbf{K}}| = 4\pi n/\lambda \sin \theta/2$ where θ equals the scattering angle, and $P(\bar{\mathbf{K}})$ equals the form factor accounting for intramolecular interference.

For the dynamic behavior, the present measurements are in the region $\bar{\mathbf{K}} < \bar{\mathbf{K}}_{max}$ with $\bar{\mathbf{K}}_{max}$ the value for which $S(\bar{\mathbf{K}})$ attains a maximal value. For short times, namely $\tau < \tau_L$, Ackerson calculated the general form of the first and second cumulant (Ackerson, 1978). τ_L is the characteristic time over which the configuration of macromolecules under the influence of the interaction forces, changes significantly. From the first cumulant, an effective diffusion coefficient can be calculated

$$D_{eff} = \frac{D_o}{S(\bar{\mathbf{K}})} \tag{2a}$$

when the hydrodynamic interaction can be neglected, and

$$D_{eff} = \frac{D_o}{S(\bar{\mathbf{K}})}\left\{1 + \frac{3}{4}[S(\bar{\mathbf{K}}) - 1]\right\} \tag{2b}$$

when the hydrodynamic force is important.

For a smaller scattering vector $\bar{\mathbf{K}} < \bar{\mathbf{K}}_{max}$ and longer times $\tau > \tau_L$ the theoretical results are less unanimous. Phillies predicted a monoexponential function for the correlation function with the diffusion coefficient given by the generalized Stokes-Einstein relation (Phillies, 1974). These results were criticized by Ackerson (Ackerson, 1978). At the same time, the interpretation of light-scattering results is complicated for many systems due to the fact that clusters are formed at higher concentrations (Bauer, 1980; Giordano et al., 1981*a*, *b*; Patkowski et al., 1979, 1980; van Helden and Vrij, 1980).

MATERIALS AND METHODS

Isolation and Preparation of Lens Proteins

The preparation of α_L-crystallins has been described elsewhere (Andries et al., 1983). For the higher concentration studies, the material from two zonal centrifugations had to be collected and concentrated to a final volume of ~1 ml. The quality of the final solutions has always been controlled by diluting a small amount of this solution to a concentration of ~1 mg/ml and measuring the diffusion coefficient of this diluted solution. It has been mostly found that the lengthy preparation procedure did not change the hydrodynamic properties and quality of the α_L-crystallin. Extra care was taken to avoid the accumulation of dust by the concentrating procedure; we have added an extra centrifugation step between the concentrating step on an Amicon concentration cell and the final concentrating on a Minicon B sample concentrator (Amicon Corp., Scientific Sys. Div., Danvers, MA), to the procedures already described before (Andries et al., 1983).

Photon Correlation Spectroscopy and Absolute Intensity Measurement of Scattered Light

The apparatus and the precautions, which have been taken during photon correlation spectroscopy and light-scattering measurements, have been described (Andries et al., 1983). Because the correlation function at higher protein concentration is no longer single-exponential, the Malvern (type 7023; Malvern Instruments, Malvern, Worchestershire, England) has been extended to 96 channels. Photon-correlation spectra have been measured at 45°, 90°, and 135° and T = 298°K. Due to the fact that the light-scattering becomes angle-dependent at high α_L concentrations, this has been measured in the angle range 30° to 140° at 10° intervals.

DATA ANALYSIS

Photon Correlation Spectroscopy

Cumulant Analysis. As a first analysis, the cumulant method proposed by Koppel (Koppel, 1972; Nieuwenhuysen, 1978) was used. In this method, no hypothesis is made about the distribution of $\Gamma = D\bar{\mathbf{K}}^2$. For a volume fraction $\phi < 0.035$ the normalized second-order cumulant, the Q factor, is <0.10 for our α_L-crystallin solutions. The deviation from 0 can be attributed to perturbations by dust particles and, therefore, Γ was obtained by an extrapolation to $Q = 0$ (Nieuwenhuysen, 1978). But from $\phi > 0.035$ on, a distinct and gradual increase in the Q value is observed and the correlation function shows a slowly decaying component. For $0.035 < \phi < 0.065$, the values for $\langle\Gamma\rangle_z$ and Q were obtained by averaging the results of ~20 correlation functions. For higher values of Q, the choice of the sample time τ becomes critical and measurements were done at different sample times and the Q factor and $\langle\Gamma\rangle_z$ were obtained by extrapolation to $\tau = 0$ (Brown et al., 1975). The high value of Q shows very clearly that in highly concentrated solutions of α_L-crystallin a complex pattern of diffusion modes is present. The cumulant method does not allow one to deduce the exact distribution function of the decay times because only a limited number of cumulants can be accurately determined and a distribution is not unambiguously characterized by its cumulants (Laiken and Printz, 1970; Bargeron, 1973). Therefore alternative analysis methods were used to arrive at a more physical interpretation of the correlation function.

Determination of $G(\Gamma, \bar{\mathbf{K}})$. To determine $G(\Gamma, \bar{\mathbf{K}})$ two approaches are possible: (*a*) postulate a form for $G(\Gamma, \bar{\mathbf{K}})$ and determine the parameters or (*b*) determine the exact inversion of the integral

$$g^1(\tau) = \int G(\Gamma, \bar{\mathbf{K}})\, e^{-\Gamma \cdot \tau}\, d\Gamma. \tag{3}$$

Sum of Exponential Functions. Polydisperse solutions with a number of discrete decay times (Lee and Chu, 1974; Bargeron, 1973, 1974; Bauer, 1980) and dynamic relaxation processes have been described as a sum of exponentials (Pusey, 1978; Jones and Caroline, 1979; Mathiez et al., 1979, 1981; Chen et al., 1977). In practice, it is difficult to extract more than two components. Two forms have been used

$$g^1(\tau) = A_1 \cdot e^{-\Gamma_1 \tau} + A_2\, e^{-\Gamma_2 \tau} \tag{4}$$

or

$$|g^1(\tau)|^2 = |A_1\, e^{-\Gamma_1 \tau} + A_2\, e^{-\Gamma_2 \tau}|^2 + B. \tag{5}$$

The fitting was performed using the damped least-squares method based on an algorithm described by Laiken (Laiken and Printz, 1970) on a VAX 11/780 computer (Digital Equipment Corp., Marlboro, MA).

Several tests were performed to decide between the two proposed functions.

(*a*) A graphical representation of the percentage of derivation between fitted and experimental values gives a visual image of the deviations. (*b*) Systematic deviations were tested by the formula proposed by Mathiez (Mathiez et al., 1979). (*c*) The R-factor significance test was performed (Hamilton, 1965; Laiken and Printz, 1970). (*d*) The uncertainty on the parameters was obtained by calculating the standard deviation on averaging over all measured curves. Because of statistical limitations, the analysis was only possible from $\sim\phi = 0.075$ on.

Exponential Sampling Method. Recently an exponential sampling method was proposed based on the eigenvalues and eigenfunctions of the Laplace transform, which should be very well suited for our problem (Ostrowsky et al., 1981). The distribution function is expanded in δ-functions

$$G[\log(\Gamma)] = \sum_{n=1}^{N} a_n \, \delta(\log\Gamma - \log\Gamma_n) \tag{6a}$$

with

$$\Gamma_{n+1} = \Gamma_n \, e^{\pi/w_m}. \tag{6b}$$

w_m determines the resolution and depends on the quality of the measurements; a_n is determined by a least-squares method. The complete distribution function is obtained by using different sets of Γ_n shifted relative to each other.

Comparison of the Three Methods. To compare the exponential sampling method and the two exponential analysis methods, the position and the height of the two maxima in the distribution function determined by the exponential sampling method were taken. The two previous methods were compared with the cumulant analysis by calculating $\langle D \rangle_z$ and Q.

Static Light Scattering. For each concentration and measuring angle the average and standard deviation was calculated, together with a number of corrections: (*a*) the volume correction $\sin\theta$; (*b* for high scattering power ($\bar{n} > 10^6$ photons/s) a correction is needed for the dead time of the photomultiplier

$$\bar{n} = \frac{\bar{n}_{obs}}{1 - \bar{n}_{obs} \cdot t}, \tag{7}$$

with $\bar{n}_{obs}$ equal to the average number of observed counts and t equals the dead time (Pike et al., 1975). (*c*) When measuring the benzene standard the dark current became important and had to be substracted; (*d*) on relating the scattered intensity I_{α_L} to the incoming intensity I_o by using a benzene standard, a refraction correction is needed to account for the difference in refractive index and depolarization

$$R_{\alpha_L} = \frac{I_{\alpha_L}}{I_{Ben}} \cdot R_{Ben} \cdot \left(\frac{n_o}{n_{Ben}}\right)^2 \cdot \frac{2}{1 + \rho_u}, \tag{8}$$

with R_{α_L} and R_{Ben} equal to the Rayleigh ratios of α_L-crystallin solutions and benzene, respectively; n_o equals the refractive index of the solution; n_{Ben} equals the refractive index of benzene; and ρ_u equals the depolarization ratio of benzene, which is 0.42 (Kerker, 1969).

RESULTS

Photon Correlation Spectroscopy

Initial Decay: Concentration Dependence. At low and moderate volume fractions $\phi < 0.035$, the correlation function is a monoexponential function and as a consequence the Q factor is small (Andries et al., 1983). However, from $\phi = 0.035$ on, important changes are noted in the diffusion behavior of the α_L-crystalline solutions. The normalized second cumulant Q deviates systematically and substantially from 0 (Fig. 1) and the correlation function shows a slowly decaying component (Fig. 2). The cumulant analysis at short times now gives the initial decay of the correlation function and can be used to calculate an effective diffusion coefficient D_{eff}, reduced to standard conditions ($T = 293°K$, ηH_2O). Fig. 3 gives the results for a systematic study of the concentration dependence of D_{eff} for α_L from bovine lenses at different angles and at a lower ($\omega = 0.08$) and at a higher ($\omega = 0.32$) ionic strength. The best higher order curves are drawn to clarify the general tendencies. At lower ionic strength ($\omega = 0.08$) the effective diffusion coefficient D_{eff} for α_L-crystallin from bovine lens cortex attains a certain maximal value and then starts to decrease. For calf cortex no decrease has been observed and at very high concentrations the D_{eff} is clearly higher. At higher ionic strength ($\omega = 0.32$) the diffusion coefficient decreases slightly for α_L from bovine lens cortex but for calf cortex there is first a slight increase, followed by a decrease. In both cases the increased ionic strength gives values for the diffusion coefficient lower than at lower ionic strength. The Q factor increases continuously from $\phi = 0.035$ on and shows no dependence on ionic strength. For a number of concentrated solutions, dilutions down to 1 mg/ml were made and photon correlation measurements and sedimentation analysis were performed. The results were the same as before (Andries et al., 1982) proving that the concentration step induces no irreversible changes.

Initial Decay: Angular Dependence. From $\phi = 0.035$ on, the initial decay of the correlation function shows a clear angular dependence. We observe a decrease of D_{eff} and an increase of Q with decreasing angle resulting in a sharper decrease for D_{eff} at $\theta = 45°$ at higher concentrations (Figs. 1 and 3). For this low-scattering angle the Q factor contains an unavoidable contribution from dust particles, which explains the large spread on the results. For $\theta \geq 90°$ the uncertainty on D_{eff} is 5% and for $\theta < 90°$ 15%. For Q, this uncertainty becomes 10 and 20%, respectively.

Determination of G (Γ, K): Sum of Exponentials. The second expression (Eq. 5) with constant baseline was clearly the best description of the results. The R test proves that the use of a fifth parameter B is significant at level 0.005. The F factor (see Mathiez et al., 1979) varied between 0.2 and 0.5 for Eq. 4 and between 0.4 and 0.9 for Eq. 5. The quality of the fits increased significantly with increasing concentration and decreasing angle. Table I shows the results for Eq. 5 for different preparations and measuring angles.

Fitting the results to an expression with more than five

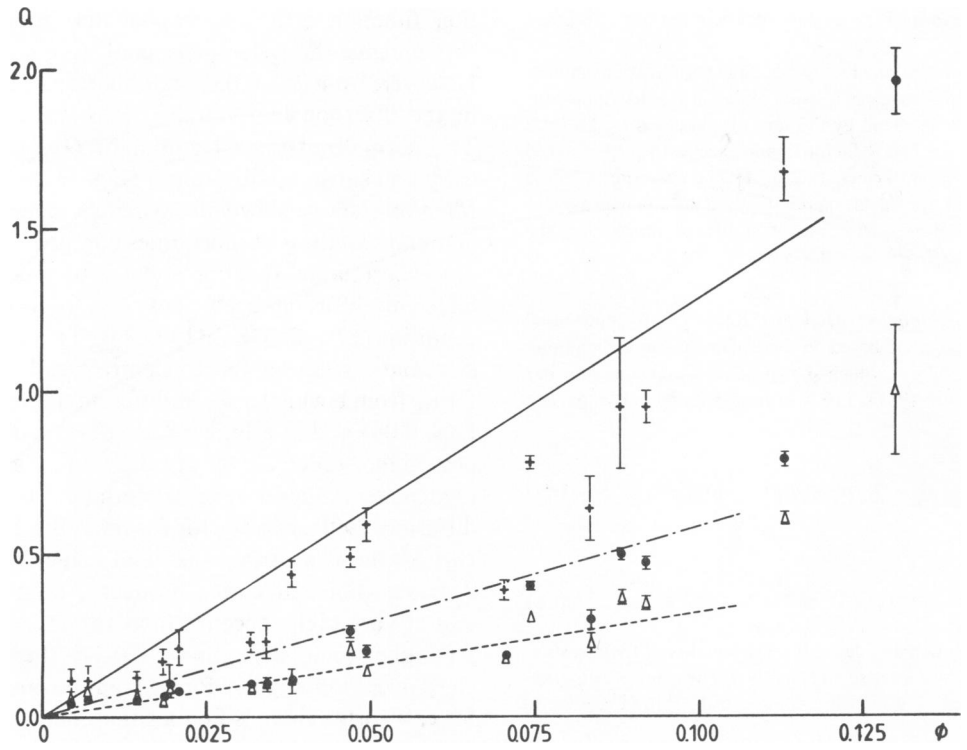

FIGURE 1 Normalized second cumulant Q of experimental correlation functions for α_L-crystallin, isolated from bovine cortical fiber cells, as a function of volume fraction ϕ; the Q/ϕ dependence for larger ϕ values is clearly angle dependent as can be expected because the slower decaying modes, which are present at higher volume fractions, are more important at smaller angles and disappear at larger angles due to the destructive interference of the scattered light. + = 45° (—), ● = 90° (— · —), and Δ = 135° (---).

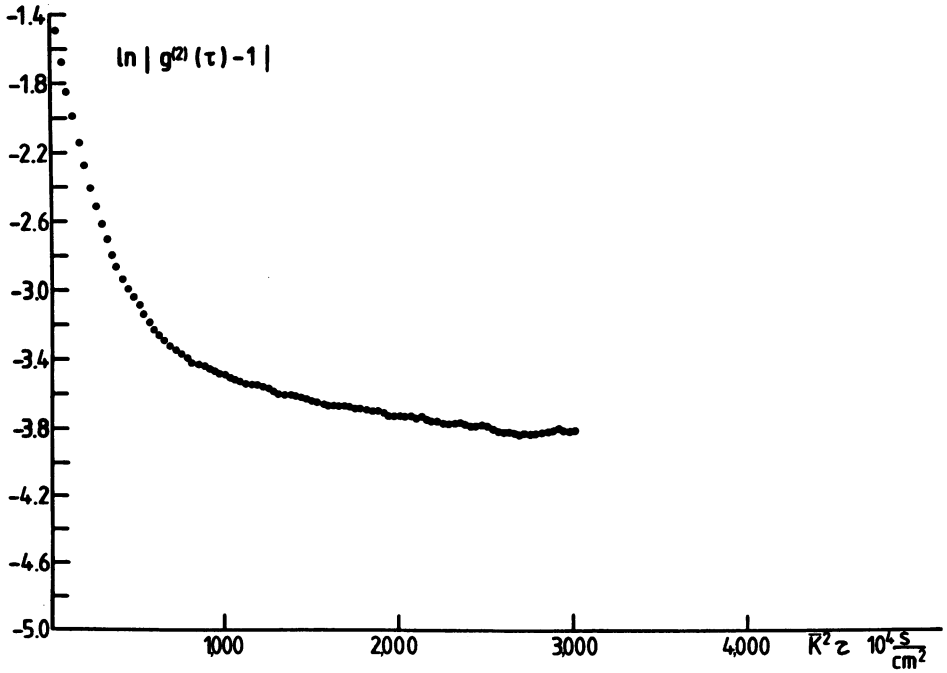

FIGURE 2 A typical example of the second-order correlation function at a volume fraction $\phi > 0.035$; the graph shows $\ln|g^2(\tau) - 1|$ as a function of $K^2\tau$ for a calf cortex α_L-crystallin solution at an ionic strength $\omega = 0.08$ and with a 96 channel digital correlator; this correlation function is clearly not a monoexponential; different methods have been used to analyze this correlation function.

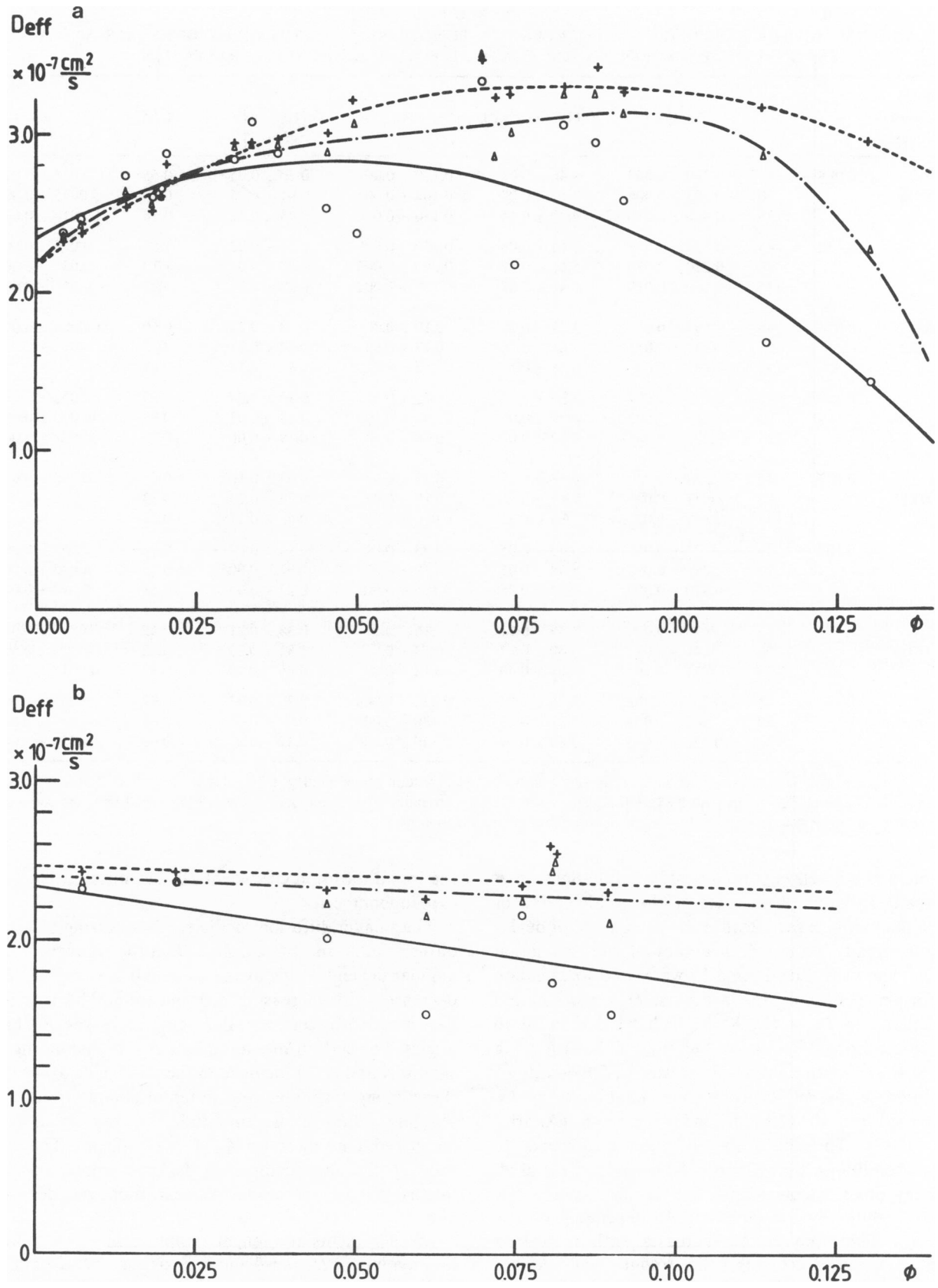

FIGURE 3 Effective diffusion coefficient for $\phi > 0.065$ α_L-crystallin isolated from bovine cortical fiber cells, and measured at (*a*) a lower ionic strength ($\omega = 0.08$) and at (*b*) a higher ionic strength ($\omega = 0.32$). The data result from measurements at three different angles: O and —, 45°; Δ and —·—, 90°; + and ---, 135°.

TABLE I

ANALYSIS OF THE EXPERIMENTAL CORRELATION FUNCTIONS AS A SUM OF EXPONENTALS AND A CONSTANT BACKGROUND FOR CORTICAL BOVINE AND CALF α-CRYSTALLIN

Material and solvent conditions	ϕ	$\theta°$	A_1	$D_1(10^{-7}\,cm^2\,s^{-1})$	A_2	$D_2(10^{-7}\,cm^2s^{-1})$	A_2/A_1	B
Bovine	0.088	45	0.270 ± 0.007	4.46 ± 0.08	0.170 ± 0.003	0.30 ± 0.05	0.65	0.011 ± 0.011
$\omega = 0.08$		90	0.353 ± 0.006	4.53 ± 0.08	0.168 ± 0.005	0.41 ± 0.06	0.48	0.0045 ± 0.0006
		135	0.400 ± 0.010	4.49 ± 0.14	0.150 ± 0.010	0.45 ± 0.12	0.38	0.0018 ± 0.0006
	0.130	45	0.120 ± 0.003	5.68 ± 0.08	0.230 ± 0.008	0.15 ± 0.02	1.84	0.065 ± 0.003
		90	0.220 ± 0.030	5.62 ± 0.12	0.260 ± 0.003	0.20 ± 0.02	1.19	0.037 ± 0.003
		135	0.200 ± 0.010	5.48 ± 0.07	0.190 ± 0.002	0.22 ± 0.01	0.92	0.011 ± 0.0006
Bovine	0.076	45	0.32 ± 0.04	3.27 ± 0.29	0.19 ± 0.02	0.38 ± 0.23	0.60	0.0088 ± 0.0022
$\omega = 0.32$		90	0.37 ± 0.05	3.05 ± 0.20	0.17 ± 0.03	0.44 ± 0.27	0.45	—
		135	0.32 ± 0.04	3.38 ± 0.17	0.22 ± 0.02	0.83 ± 0.18	0.69	—
	0.158	45	0.170 ± 0.007	3.69 ± 0.07	0.21 ± 0.01	0.14 ± 0.04	1.23	0.052 ± 0.009
		90	0.236 ± 0.003	3.70 ± 0.05	0.196 ± 0.004	0.18 ± 0.03	0.83	0.015 ± 0.002
		135	0.26 ± 0.06	3.62 ± 0.02	0.19 ± 0.04	0.19 ± 0.06	0.72	0.0083 ± 0.003
Calf	0.083	45	0.34 ± 0.02	4.38 ± 0.12	0.17 ± 0.01	0.63 ± 0.12	0.51	0.090 ± 0.0030
$\omega = 0.08$		90	0.31 ± 0.02	4.19 ± 0.26	0.10 ± 0.02	0.74 ± 0.23	0.33	—
		135	0.33 ± 0.02	3.86 ± 0.22	0.070 ± 0.02	0.48 ± 0.27	0.21	—
	0.158	45	0.24 ± 0.01	5.43 ± 0.05	0.23 ± 0.01	0.14 ± 0.02	0.96	0.058 ± 0.004
		90	0.287 ± 0.003	5.42 ± 0.05	0.19 ± 0.02	0.191 ± 0.005	0.65	0.015 ± 0.002
		135	0.320 ± 0.002	5.37 ± 0.05	0.186 ± 0.003	0.22 ± 0.02	0.58	0.010 ± 0.001
Calf	0.122	45	0.38 ± 0.02	3.59 ± 0.11	0.16 ± 0.01	0.33 ± 0.21	0.42	0.0068 ± 0.0020
$\omega = 0.32$		90	0.41 ± 0.04	3.60 ± 0.27	0.13 ± 0.05	0.36 ± 0.20	0.32	0.0010 ± 0.0006
		135	0.41 ± 0.16	3.64 ± 0.40	0.13 ± 0.03	0.45 ± 0.10	0.33	0.0011 ± 0.0006
	0.145	45	0.230 ± 0.003	3.76 ± 0.04	0.230 ± 0.004	0.20 ± 0.03	0.99	0.045 ± 0.005
		90	0.260 ± 0.003	3.82 ± 0.05	0.180 ± 0.004	0.28 ± 0.04	0.68	0.017 ± 0.002
		135	0.220 ± 0.003	3.84 ± 0.04	0.130 ± 0.003	0.32 ± 0.03	0.60	0.0038 ± 0.005

Analysis of the experimental correlation functions as a sum of exponentials and a constant background $|g^1(\tau)|^2 = |A_1 e^{-\Gamma_1\tau} + A_2 e^{-\Gamma_2\tau}|^2 + B$ for cortical bovine and calf α_L-crystallin at lower ($\omega = 0.08$) and higher ($\omega = 0.32$) ionic strength, at three measuring angles (45°, 90°, 135°), and some typical volume fractions ϕ (other volume fractions have been measured but are not mentioned).

parameters is not relevant because the fluctuations on B are already rather high because of the incalculation of random fluctuations and because the percentage of deviation falls already within the accuracy of the correlation function. The quantities Γ_1 and Γ_2 were used to calculate the diffusion coefficients, the larger one $D_1 = (\Gamma_1/\overline{K}^2)$ and the smaller one $D_2 = (\Gamma_2/\overline{K}^2)$, which were reduced to standard conditions. For the calculation of the scattering vector $\overline{K}$, the refractive index of H_2O was used. Corrections for an increase of n with concentration are at most 2 or 3% as estimated from the refractive index increment (Andries et al., 1982). To reduce the diffusion coefficients to standard conditions, the viscosity of the solvent was used. The decay times or equivalently the diffusion coefficients D_1 and D_2 differ by a factor 4 to 40 depending on the conditions. The ratio D_1/D_2 increases with increasing concentration and decreasing ionic strength and is higher for bovine than for calf lens. The larger diffusion constant D_1 increases with increased concentration and, very important, the angular dependence that was very pronounced for the initial diffusion coefficient D_{eff} has disappeared within experimental error.

The smaller diffusion coefficient D_2 referring to a slower diffusing unit and the baseline B on the contrary are still angular dependent. D_2 increases with increasing angle and decreases with increasing concentration. The baseline B increases with concentration but decreases at higher angles. For certain measurements B was fluctuating considerably and is not included in the table. Due to the use of the clipping technique and different sample times τ, the absolute values of the amplitudes A_1 and A_2 cannot be compared, only the ratio A_2/A_1 is significant. The amplitude of the slow component becomes more and more important with increasing concentration and decreasing angle.

Measurements at a longer sample time τ give a slightly lower value for D_2 and B and comparison of D_2 from Eqs. 4 and 5 show that D_2 from Eq. 4 is lower than D_2 from Eq. 5. Together with the angular dependence, this suggests that the second component cannot be described by a monoex-

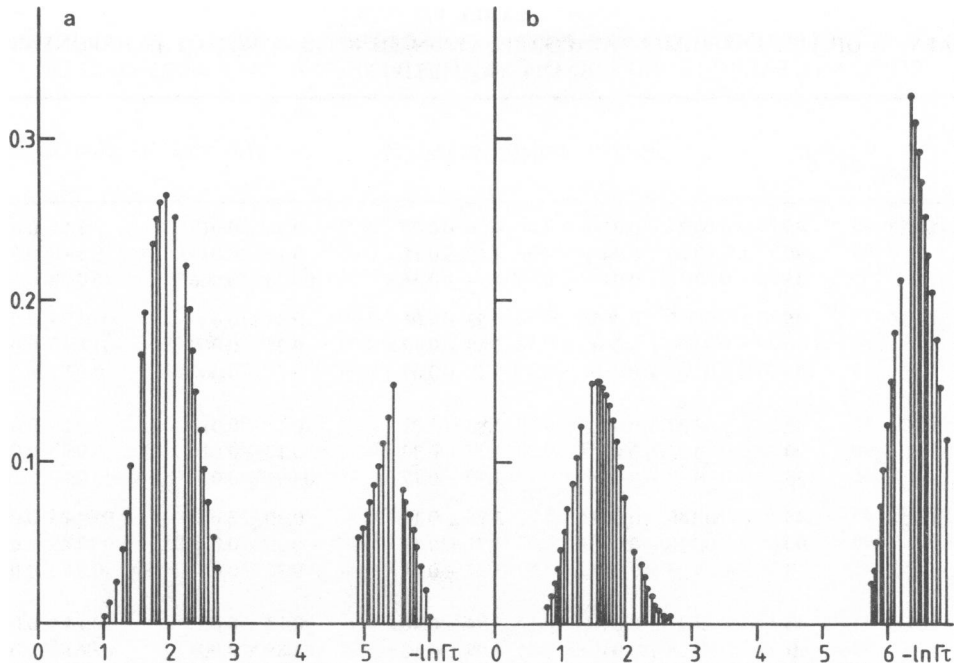

FIGURE 4 Distribution function $G(\Gamma)$ obtained with the exponential sampling method according to Eq. 6. The figure gives the amplitude A as a function of $-\ln \Gamma\tau$. The figure relates to measurements at 45°; *a* results from calf cortical α_L-crystallin solutions at low ionic strength and at a volume fraction ϕ of 0.083 and *b* at a volume fraction ϕ of 0.158.

ponential function but is probably a distribution of slowly decaying components.

Exponential Sampling Method. The exponential sampling method confirms that the correlation function contains two clearly separated decay modes. The concentration and the angular and the ionic strength dependence are similar as for the two exponential analysis method. Fig. 4 shows the distribution function for one angle and two volume fractions. To compare the results with two exponential analysis method the position and the amplitude of the maxima were determined (Table II). The main difference is that $D_{2,max}$ of the exponential sampling method is lower by at least 50%. This can be explained by the fact that a broad range of slowly decaying components is present, part of which is described by the constant baseline B of Eq. 5.

Comparison of the Three Methods. Comparison of the values $\langle D \rangle_z$ and Q calculated from the initial decay, with the calculated values from the more elaborated analyses shows that the agreement is good with the exponential sampling method but the values for D_2 from the two exponential analyses are too high and Q to low because it is impossible to take into account the components covered by the baseline B (Table III).

Statical Light Scattering: Concentration Dependence. Fig. 5 shows as an example the scattered intensity as a function of volume fraction ϕ for different scattering angles (θ = 45°, 90°, 135°), at low ionic strength for bovine α_L-crystallin. The scattered intensity I_{θ,α_L} for θ = 90° and 135° for bovine α_L-crystallin at low ionic strength increases as a function of the volume fraction until ϕ = 0.040 and then decreases. For θ = 45° a continuous increase is observed although the fluctuations are large for this angle. For $\theta \geq 90$ the experimental uncertainty is ~10% and increases to 20% for smaller angles. Calf α_L-crystallins give the same results as bovine ones. Similar measurements at higher ionic strength show a similar behavior but for θ = 45°, also a decrease is observed at very high volume fractions. The maximum is 20 to 30% higher than at lower ionic strength but the decrease at higher concentrations is more pronounced. For all measuring conditions, the scattered intensity per concentration unit decreases from $\sim\phi$ = 0.010 on.

Angular Dependence. For $\phi < 0.035$ no angular dependence could be observed (Andries et al., 1983) but from ϕ = 0.035 on, a clear and increasing forward scattering is observed (Fig. 6). The ionic strength has little influence on this effect.

DISCUSSION

Interpretation of the Experimental Results

In a previous article (Andries et al., 1983) we showed that the concentration dependence of the diffusion coefficient

TABLE II
ANALYSIS OF THE EXPERIMENTAL CORRELATION FUNCTIONS WITH THE EXPONENTIAL SAMPLING METHOD

Material and solvent conditions	ϕ	$\theta°$	A_1	$D_1(10^{-7}cm^2s^{-1})$	A_2	$D_2(10^{-7}cm^2s^{-1})$	A_2/A_1
Bovine	0.088	45	0.24 ± 0.01	4.56 ± 0.35	0.16 ± 0.01	0.12 ± 0.01	0.67
$\omega = 0.08$		90	0.26 ± 0.04	4.48 ± 0.18	0.14 ± 0.01	0.19 ± 0.02	0.54
		135	0.38 ± 0.01	4.29 ± 0.36	0.120 ± 0.006	0.26 ± 0.03	0.32
	0.130	45	0.098 ± 0.005	5.53 ± 0.06	0.34 ± 0.02	0.045 ± 0.02	3.47
		90	0.200 ± 0.004	5.68 ± 0.12	0.28 ± 0.009	0.086 ± 0.007	1.40
		135	0.200 ± 0.010	5.48 ± 0.07	0.19 ± 0.002	0.22 ± 0.01	0.92
Bovine	0.076	45	0.27 ± 0.04	2.83 ± 0.21	0.15 ± 0.01	0.12 ± 0.02	0.56
$\omega = 0.32$		90	0.33 ± 0.05	2.75 ± 0.33	0.12 ± 0.01	0.26 ± 0.07	0.36
		135	0.32 ± 0.05	2.70 ± 0.17	0.098 ± 0.02	0.29 ± 0.06	0.43
	0.158	45	0.140 ± 0.007	3.95 ± 0.12	0.30 ± 0.02	0.044 ± 0.001	2.14
		90	0.220 ± 0.006	3.71 ± 0.12	0.20 ± 0.02	0.089 ± 0.003	0.91
		135	0.25 ± 0.01	3.37 ± 0.01	0.20 ± 0.02	0.11 ± 0.01	0.80
Calf	0.083	45	0.27 ± 0.04	3.84 ± 0.46	0.13 ± 0.02	0.14 ± 0.03	0.48
$\omega = 0.08$		90	0.28 ± 0.03	4.09 ± 0.18	0.089 ± 0.006	0.063 ± 0.021	0.32
		135	0.31 ± 0.01	4.03 ± 0.09	0.10 ± 0.02	0.26 ± 0.02	0.32
	0.158	45	0.15 ± 0.01	6.12 ± 0.43	0.31 ± 0.08	0.048 ± 0.002	2.07
		90	0.23 ± 0.01	5.85 ± 0.46	0.23 ± 0.01	0.10 ± 0.02	1.00
		135	0.347 ± 0.005	5.76 ± 0.43	0.175 ± 0.005	0.12 ± 0.008	0.47
Calf	0.122	45	0.30 ± 0.03	3.64 ± 0.28	0.14 ± 0.01	0.13 ± 0.02	0.47
$\omega = 0.32$		90	0.36 ± 0.05	3.43 ± 0.18	0.11 ± 0.02	0.26 ± 0.07	0.31
		135	0.34 ± 0.03	3.53 ± 0.14	0.097 ± 0.008	0.25 ± 0.03	0.29
	0.145	45	0.15 ± 0.01	3.76 ± 0.11	0.30 ± 0.01	0.068 ± 0.013	2.0
		90	0.20 ± 0.01	3.85 ± 0.14	0.120 ± 0.006	0.18 ± 0.03	0.67
		135	0.18 ± 0.02	3.85 ± 0.10	0.12 ± 0.01	0.18 ± 0.01	0.67

D_1 and D_2 correspond to the diffusion coefficient of the maxima in the distribution function $G(\Gamma, K)$.

for $\phi < 0.035$ can be described by a linear relationship $D = D_0(1 + \alpha\phi)$. This concentration dependence is due to the direct interaction with the neighboring macromolecules and the indirect hydrodynamic interaction. These two contributions could be measured separately by static light scattering and by fluorescence correlation spectroscopy, which measures the tracer diffusion coefficient. Combination of these two results in the generalized Stokes-Einstein relation gave the photon correlation diffusion coefficient D_m within experimental error although there was a systematic overestimation of D_m. The interaction could be described by a hard sphere potential modified by an electrostatic repulsion term.

For the higher volume fractions studies in this article, no tracer measurements were performed but we tried to match our measurements with the formulas deduced by Ackerson (Eqs. 2a and b). Fig. 7 shows D_{eff} from the initial decay of the correlation function together with the calculated values. For $\phi < 0.035$ the results are properly described but for higher volume fractions the results are largely overestimated a possible reason being that the two body potential used to derive the formula is no longer valid. For a hard sphere potential (Nieuwenhuis et al., 1981) and for an electrostatic repulsion (Doty and Steiner, 1952) an angular dependence in the scattered light can be expected with $I_{45°} < I_{135°}$ but should be rather weak. Clearly the light scattering and diffusion behavior at higher volume fractions can no longer be described in terms of a simple interaction potential and with first-order approximations.

Interpretation of D_1. The diffusion coefficient D_1, calculated from the fast decaying component of the correlation function, shows the same linear increase with volume fraction as the diffusion coefficient for $\phi < 0.035$ (Fig. 7) and is not angular dependent. Therefore, it must be interpreted as the collective relaxation of the free but interacting α_L-crystallins.

Interpretation of D_2. Both the angular dependence of the scattered intensity as well as the angular dependence of A_2 prove the formation of large scattering units. The angular dependence of D_2 and different experimental results due to the various analysis techniques and measuring times lead to the conclusion that a broad range

TABLE III
COMPARISON OF PARAMETERS $\langle D \rangle$ AND Q

Material and solvent conditions	ϕ	$\theta°$	Cumulant analysis		Sum of two exponentials analysis		Exponential sampling method	
			$D_z(10^{-7}cm^2s^{-1})$	Q	$D_z(10^{-7}cm^2s^{-1})$	Q	$D_z(10^{-7}cm^2s^{-1})$	Q
Bovine	0.088	45	2.94	0.96	2.82	0.52	2.86	0.86
$\omega = 0.08$		90	3.26	0.50	3.20	0.36	3.37	0.44
		135	3.41	0.37	3.39	0.28	3.64	0.43
	0.130	45	1.41	4.0 ± 0.5	2.10	1.58	1.33	3.53
		90	2.27	1.95	2.67	1.02	2.54	1.67
		135	2.94	1.00	2.96	0.79	2.84	1.15
Bovine	0.076	45	2.18	0.95	2.18	0.41	2.16	1.03
$\omega = 0.32$		90	2.24	0.38	2.24	0.29	2.35	0.42
		135	2.34	0.39	2.36		2.38	0.37
	0.158	45	1.36	3.0 ± 0.3	1.73	1.04	1.38	2.65
		90	2.02	1.1	2.10	0.70	2.08	1.03
		135	2.18	0.82	2.17	0.62	2.22	0.78
Calf	0.083	45	3.00	0.65	3.03	0.31	3.09	0.50
$\omega = 0.08$		90	3.25	0.30			3.28	0.25
		135	3.32	0.23	3.26	0.15	3.54	0.40
	0.158	45	2.30	2.00	2.76	0.91	2.41	1.87
		90	3.18	0.90	3.31	0.60	3.32	0.86
		135	3.42	0.74	3.38	0.53	3.63	0.76
Calf	0.122	45	2.79	0.80	2.63	0.32	2.72	0.53
$\omega = 0.32$		90	2.80	0.75	2.82	0.24	2.91	0.36
		135	2.86	0.65	2.86	0.23	2.83	0.27
	0.145	45	1.78	1.80	1.94	0.81	1.75	1.65
		90	2.32	0.75	2.34	0.54	2.45	0.92
		135	2.48	0.65	2.43	0.46	2.66	0.65

Comparison of the parameters $\langle D_z \rangle$ and Q determined from the initial decay using the cumulant analysis (expression 5), and the same parameters calculated from the results of the sum of two exponential analysis (Eq. 5), and from the exponential sampling method (Eqs. 6a and b).

of large scattering units is present. A contribution due to collective relaxation processes cannot be excluded. With this in mind we estimated the size of the scattering units in two independent ways.

(*a*) We use the Stokes-Einstein relation $R_H = (k\,T/6\,\pi\,\eta\,D_2)$ where η is equal to the viscosity of the solvent. Bauer (Bauer, 1980) suggested that large clusters do not feel the viscosity of the solvent but rather the viscosity due to the surrounding free macromolecules and the solvent. In this case it is intrinsically impossible to determine η.

(*b*) We assume that the scattered intensity is a superposition of the light scattered by the free α_L-crystallins and the large units and that no interference occurs between the light scattered at these two types; therefore, we obtain $R_\theta = \kappa \cdot c \cdot M_2 \cdot S(\bar{K}) \cdot P(\bar{K}) + \kappa\, c^* M^*_r S^*(\bar{K})\, P^*(\bar{K})$. The symbols with an asterisk denote the parameters related to the large scattering units. We also assume that $S^*(\bar{K})$ and $P(\bar{K})$ are almost equal to 1 and that $S(\bar{K})$ is nearly angular independent. If we assume that for $\theta \geq 120°$ $P^*(\bar{K}) \rightarrow 0$, we can separate the two contributions (van Helden and Vrij, 1980).

Using the Guinier approximation $P^*(\bar{K}) \sim e^{-\bar{k}^2 \cdot R_g^2/3}$ we obtain the radius of an equivalent sphere $R = \sqrt{5/3}\,Rg$ of the large units.

$\ln [(I_{\theta,\alpha_L}/I_{90°,Ben}) - (I_{140°,\alpha_L}/I_{90°,Ben})]$ as a function of $\bar{K}^2$ could be well described by a linear function (Fig. 8).

Table IV shows the results for those procedures used in *a* and *b* given above. Of course large deviations are observed, the values of the two exponential analysis are generally lower because of the polydispersity. From these values we can calculate an estimate for the number of individual α_L-crystallins contained in one cluster, e.g., for $\phi = 0.085$ and $R = 137$ nm, we get $\sim 10^3$ units. These dimensions together with the reversible character of the large-scattering units point to the formation of clusters rather than to aggregation with specific binding. This is also consistent with biochemical studies of α_L-aggregation (Siezen and Owen, 1983). The clear relative increase in the amount of clusters with concentration and decreasing ionic strength favors the hypothesis of cluster formation due to a secondary minimum in the potential as the net effect of electrostatic repulsion and Van der Waals attraction (Bauer,

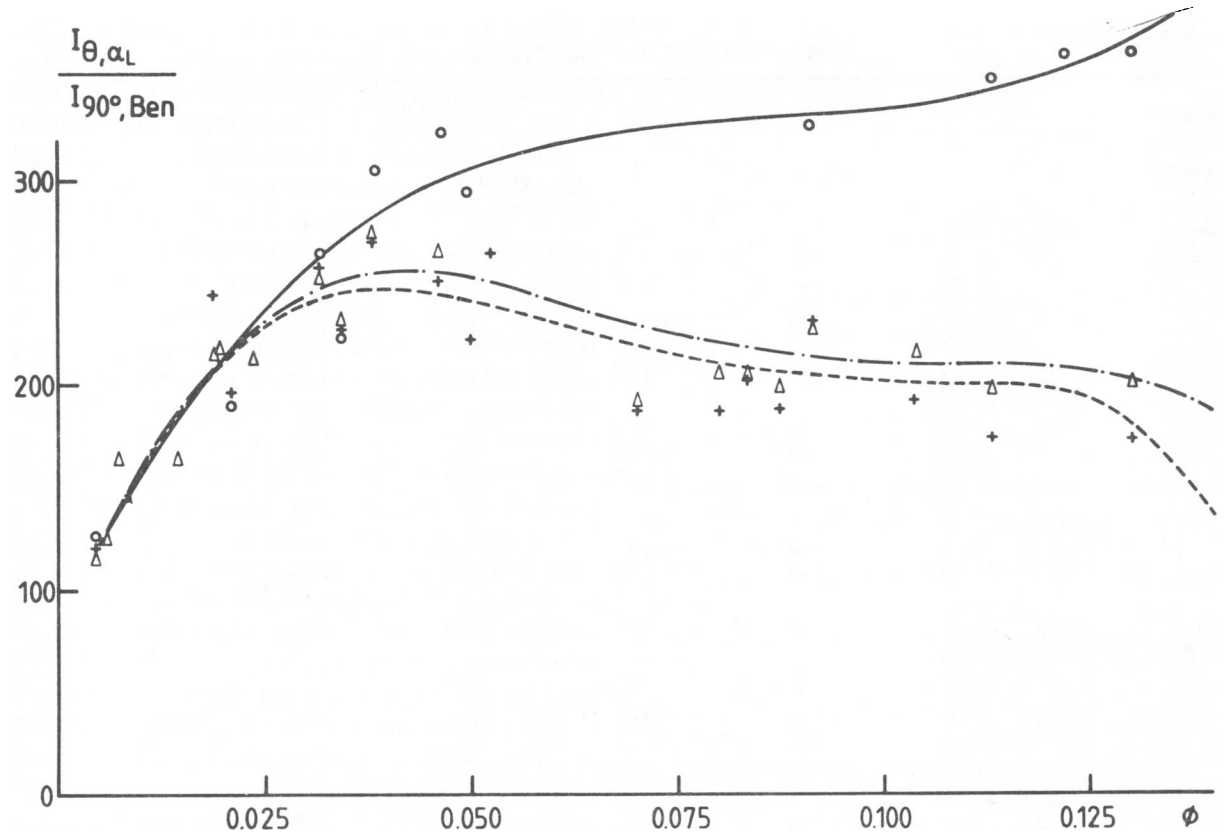

FIGURE 5 Scattered intensity by α_L-crystallin solutions, isolated from bovine cortical fiber cells, relative to benzene; the figure shows the results at three different angles (O and — at 45°; Δ and —·— at 90°; + and --- at 135°) as a function of volume fraction ϕ of the protein.

1980). This would also explain why cluster formation becomes more important for older α_L-crystallins isolated from 3 y old bovine lens cortex as compared with α_L-crystallins from 6 mo old calf lens cortex because it is known that α_L-crystallin molecules acquire more charges with aging (Van Kamp et al., 1973).

Biological Interpretation

For the normal lens a turbidity

$$r = -\frac{1}{y} \ln \frac{I_o - I_{tot}}{I_o},$$

between 0.020 mm^{-1} and 0.025 mm^{-1} was observed (Clark and Benedek, 1980), where y equals the path length, I_o equals the incident light intensity, and I_{tot} equals the total scattered intensity. From $\sim r = 0{,}040$ mm^{-1} the lens can be considered opaque.

When no angular dependence is observed, a simple relationship exists between the turbidity and the measured Rayleigh ratio R_θ. For polarized light $r = (8\pi R_\theta/3)$ (Marshall, 1978). For higher volume fractions $\phi > 0.035$ where a clear angular dependence is observed we assumed the same angular relationship for all planes rotated around the axis of the incoming beam. The total scattered intensity was obtained by the following numerical integration

$$\frac{I_{tot}}{I_0} = \left[\int_0^{2\pi}\int_0^{\pi} dS \cdot \sin^2\theta \,(be^{-R_g^2 \cdot \bar{K}^{2/3}} + c)\right] \cdot R_{Ben}\left(\frac{n_0}{n_{Ben}}\right)^2 \frac{2}{1+\rho_u}, \quad (9)$$

with dS equal to $2\pi \sin\theta \cdot d \cdot d\phi_1$, which equals the surface element; $\sin^2\theta$ equals the angular dependence of polarized light (Marshall, 1978); ϕ_1 equals the angle between the incident beam and the projection of the scattered beam on the plane perpendicular to the polarization direction (equal to the horizontal plane); θ equals the angle between the direction of polarization and scattered beam.

Table V gives the turbidity at different volume fractions. We can see that although the α_L-crystallin solutions are a very simplified model system for the eye lens, they form a transparent system even at the in vivo concentration. At the same time clusters are formed that increase the scattering but do not disturb the transparency in our systems.

Short-range and/or Long-range Interactions?

Delaye and co-workers have recently published x-ray and light-scattering data on total cytoplasma of calf lenses and

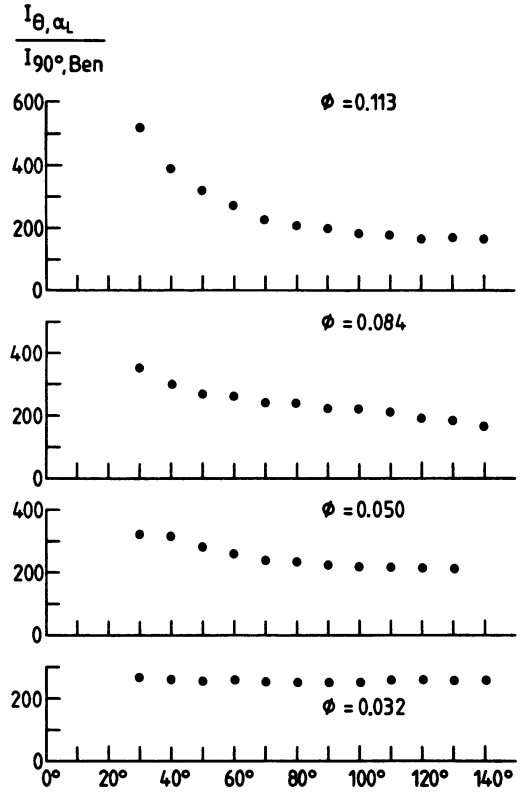

FIGURE 6 Scattered intensity of α_L-crystallin solutions, isolated from bovine cortical fiber cells, relative to benzene; the figure shows the results at angles between 30° and 140° and at different volume fractions ϕ.

on more diluted solutions of this cytoplasma, in this way they concentrated on both the ideal and the physiological solutions (Delaye and Tardieu, 1983; Delaye and Gromiec, 1983). This system is of course very close to our model system; in some ways it is closer to reality, but it does not allow for a rigorous description due to the heterogeneity of the system. The experimental results are very similar for light scattering and photon correlation spectroscopy. At higher concentration, a slowly relaxing component appears. There is one important difference. Our model clearly shows an angle dependence for light scattering, which indicates the formation of units the size of the wavelength of the light. The same asymmetry has also been observed by Delaye et al. in a similar study on the cytoplasma of the lens nucleus of calf lenses (Delaye et al., 1982). There, they interpret this asymmetry as the formation of correlated areas in the solution that precedes cold cataract formation. It is tempting to describe the clusters we observe in the highly concentrated solutions of α_L in the same way—as the formation of correlated parts in the solution—and in this way we interpret the existence of local areas of order over larger distances. The presence of β- and γ-crystallins do probably prevent the formation of this local ordering. It is not known to what extent this phenomenon is related to the synchronous observation of the disappearance of γ-crystallins in older lenses (Augusteyn, 1981) and to the increase of light scattering, which can be related to the appearance of larger scattering units.

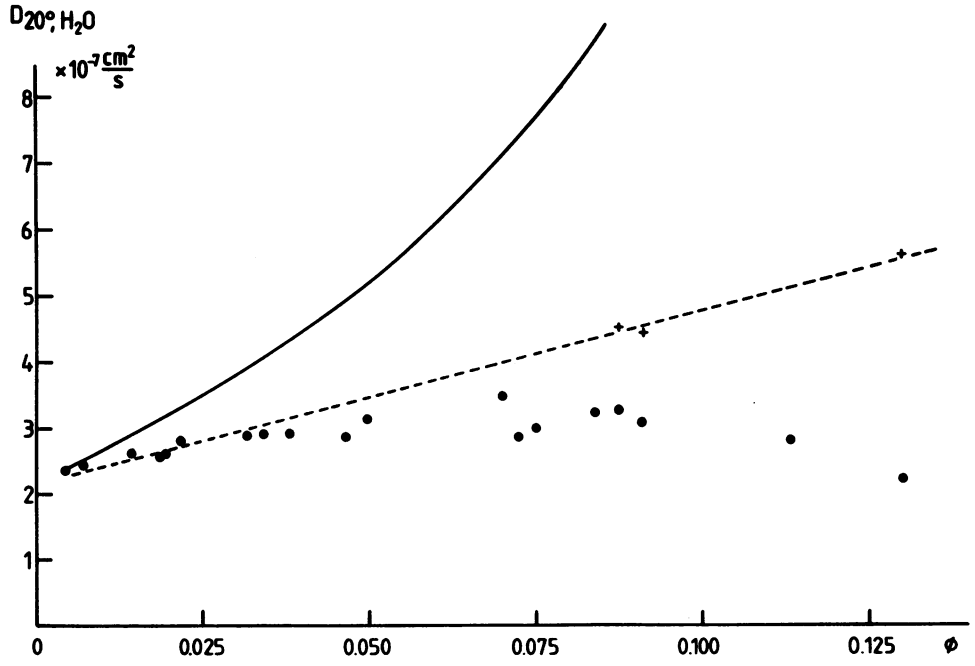

FIGURE 7 Effective diffusion coefficient D_{eff} (●) calculated from the first-order cumulant, as compared to the diffusion coefficient D_1 (+ and ---), which can be caluclated from the sum of exponentials analysis, and the theoretical diffusion coefficient (—), which can be calculated accepting a hard-sphere potential and hydrodynamical interaction $D_{eff} = (D_o/S[\overline{K}])\{1 + 3/4\,[S(\overline{K}) - 1]\}$ (Ackerson, 1978). At small volume fractions the effective diffusion coefficient D_{eff} is well described by the Ackerson relation but at higher volume fractions largely overestimated. The large diffusion coefficient D_1 from the two-exponential analysis follows the same linear dependence on concentration as D_{eff} at low volume fraction but is still overestimated by the Ackerson formula.

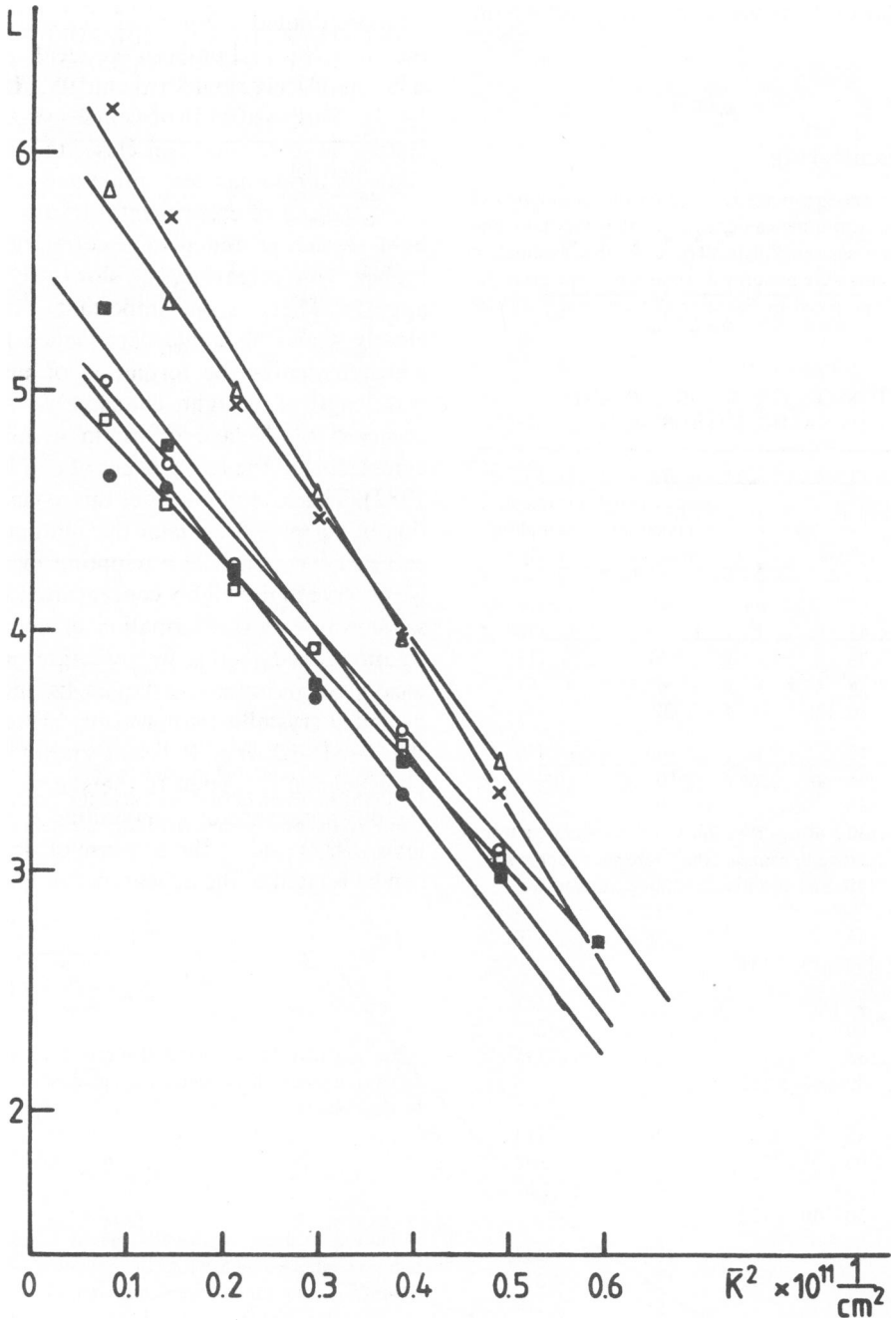

FIGURE 8 Estimation of the size of the clusters present at high α_L-crystallin concentrations using the Guinier expression $L = \ln [(I_{\theta,\alpha L}/I_{90°,Ben}) - (I_{140°,\alpha L}/I_{90°,Ben})]$ gives the logarithm of the contribution due to larger scattering units, if one accepts that $I_{140°,\alpha L}$ gives the constant scattered intensity, related to the presence of the smaller, single α_L-crystallins. From the curves L vs. $\bar{K}^2$, the radius of gyration can be calculated at different volume fractions of the α_L-crystallins. The different curves correspond to different volume fractions ϕ as follows: □, 0.047; ●, 0.050; ■, 0.080; ○, 0.083; ×, 0.105; Δ, 0.114.

CONCLUSION

The interactions between the α_L-crystallins induce correlations that give rise to a decreasing scattered intensity per concentration unit, which results in a transparent solution even at the in vivo concentration. Higher ionic strengths increase the scattered intensity but very high values are needed to disturb transparency. At the same time for volume fractions $\phi > 0.035$, clusters are formed, which result in a slowly decaying component in the photon correlation function and increased forward scattering. The formation of clusters is reversible with dilution; formation decreases at higher ionic strength and when younger material, i.e., for α_L-crystallins from calf lens cortex is used. Notwithstanding the strong scattering power of these clusters the α_L-crystallin solutions at volume fractions of

0.150, which is similar to the in vivo concentration, remain transparent.

APPENDIX

Multiple Scattering

The interpretation of our measurements is based on the assumption of single scattering. Multiple scattering can drastically alter the static and dynamic properties of the scattered light. To verify this assumption depolarization measurements were performed. To interpret our measurements we used the theory proposed by Sørensen (Sørensen et al., 1976; Sørensen et al., 1978) assuming that it is a good approximation for interacting particles like ours. He proposes a relation between the average number of scatterings per photon n and the depolarization ratio $\rho_v = (I_\perp/I_{//})$, where v indicates the vertically polarized incident light; $I_\perp$ represents the scattered intensity with polarization direction perpendicular to the direction of polarization of the incident light; $I_{//}$ represents the scattered intensity with polarization parallel to the polarization direction of the incident light

$$\rho_v(n) = \frac{\sum_{n=1}^{\infty} \frac{\rho_n}{1+\rho_n} \cdot P(n)}{\sum_{n=1}^{\infty} \frac{1}{1+\rho_n} \cdot P(n)}, \qquad \text{(A1)}$$

where ρ_n equals the depolarization ratio for n-times scattered light; $P(n)$ equals the probability of detecting a photon after n-scattering events given by the Poisson distribution

$$P(n) = \frac{\mathbf{n}^{-n} \cdot \mathbf{e}^{-n}}{n!}.$$

The initial decay of the depolarized correlation function is angular independent. This means that the relation $\Gamma = D\bar{\mathbf{K}}^2$ no longer holds. For light scattered n-times, Sørensen becomes $\Gamma_n = n\Gamma_1$ (90°). Experimentally the polarization of the scattered light was analysed with a beam-splitting cube before the photomultiplier (type PBS5-1; CVI Laser Corp., Albuquerque, NM).

The experimental set-up was checked by measuring the depolarization ratio of benzene. The contribution of the intrinsic anisotropy of the α_L-crystallin was determined by measurements at a 1 mg/ml concentration where multiple scattering has certainly no influence. For a series of concentrations the depolarization ratio ρ_v was measured at $\theta = 90°$. For one solution the angular dependence of the static and dynamic light scattering was recorded in the I_{vv} and $I_{v(v+h)}$ configuration, i.e., vertically polarized incident light and detection of the parallel component of the scattered light only or parallel and perpendicular components together, respectively. The intrinsic depolarisation ratio of α_L-crystallin was very small, $\rho_v = 0.0003$. Comparison between the results in the I_{vv} and $I_{v(v+h)}$ mode gave no difference.

Table VI gives the value for ρ_v (90°) at different volume fractions together with the average number of scatterings n calculated with the aid of Eq. A1. On average the depolarization was 0.25%, which means an

TABLE IV
CALCULATION OF THE RADIUS R AND HYDRODYNAMIC RADIUS R_H

Material and solvent conditions	ϕ	θ°	R	R_H sum of two exponential analysis	R_H exponential sampling analysis
			nm	*nm*	*nm*
Bovine	0.088	45		70	176
$\omega = 0.08$		90		51	111
		135		47	81
		30–140	137		
	0.130	45		140	468
		90		105	245
		135		96	191
		30–140	194		
Bovine	0.076	45		56	179
$\omega = 0.32$		90		49	83
		135		26	74
		30–140	134		
	0.158	45		153	488
		90		119	241
		135		113	195
		30–140	135		
Calf	0.083	45		34	153
$\omega = 0.08$		90		29	340
		135		45	83
		30–140	122		
	0.158	45		153	447
		90		113	214
		135		98	179
		30–140	155		
Calf	0.122	45		65	165
$\omega = 0.32$		90		60	83
		135		48	86
		30–140	109		
	0.145	45		107	315
		90		77	119
		135		67	119
		30–140	149		

Calculation of the radius R of the equivalent sphere for the larger scattering units from the light scattering measurements in the angle range 30°–140° using the Guinier approximation; calculation of the hydrodynamic radius R_H of the equivalent sphere from the Stokes-Einstein relation introducing the smaller diffusion coefficient D_2 using the sum of two exponential analysis or the exponential sampling analysis method.

TABLE V
CALCULATION OF THE TURBIDITY r OF SOME HIGHLY CONCENTRATED α_L SOLUTIONS FROM THE EXPERIMENTAL LIGHT SCATTERING IN THE ANGLE RANGE 30–140° USING EQ. 9

Material and solvent conditions	ϕ	$1 - \frac{I_{tot}}{I_0}$	r*
Bovine	0.088	0.91	0.0091
$\omega = 0.08$	0.130	0.79	0.024
Bovine	0.076	0.89	0.012
$\omega = 0.32$	0.158	0.85	0.016
Calf	0.083	0.94	0.0066
$\omega = 0.08$	0.158	0.93	0.0074
Calf	0.122	0.94	0.0063
$\omega = 0.32$	0.145	0.89	0.012

*For 1 cm path length.

TABLE VI
DEPOLARIZATION RATIO ρ_v AND CORRESPONDING MEAN NUMBER OF SCATTERING EVENTS, n, FOR EACH SCATTERED PHOTON

ϕ	$\rho_v = I_{vh}/I_{vv}$	n	I, double scattered/ total intensity	I, triple scattered/ total intensity
0.038‡	0.00069	0.012	0.006	0.00024
0.048*	0.0026	0.046	0.023	0.00035
0.075‡	0.0028	0.051	0.0255	0.00011
0.145*	0.00157	0.028	0.014	0.00003
0.158*	0.0024	0.042	0.021	0.00007

The depolarization ratio, ρ_v, and the corresponding mean number of scattering events, n, for each scattered photon are calculated using Eq. A1. The relative contribution of double-scattered light is calculated using the ratio $P(2)/P(1)$ and the relative contribution of triple-scattered light is calculated using the ratio $P(3)/P(1)$.
*Calf α_L-crystallin.
‡Bovine α_L-crystallin.

average number of scattering events per photon of $\bar{n} = 0.040$. The ratios $P(2)/P(1)$ and $9I_{vh}/I_{vv} - 8I_{vh}$ both show that the double-scattered light is only 2% of the single scattered. The contribution of the triple-scattered light diminishes to 0.03%. We can conclude that double-scattered light contributes little to the total scattered light but its influence on the angular dependence of the static and dynamic light scattering falls within experimental error and our conclusions need not be adapted.

We thank T. Aerts and J. De Block for their skillful technical assistance and Dr. M. Rabaey and Dr. P. Nieuwenhuysen for constructive discussions. C. Andries thanks the Institute for Scientific Research in Industry and Agriculture (IWONL) for a fellowship.

This research was supported by grants from the Fund for Joint Basis Research (FKFO) and the Fund for Medical Scientific Research (FGWO). This research was performed within the framework of Eurage (EEC concerted action on cellular aging and diseases).

Received for publication 17 October 1983 and in final form 9 October 1984.

REFERENCES

Ackerson, B. J. 1978. Correlation for interacting Brownian particles II. *J. Chem. Phys.* 69:684–690.

Andries, Chr., H. Backhovens, J. Clauwaert, J. De Block, Fr. De Voeght, and Chr. Dhont. 1982. Physical-chemical studies on bovine eye lens proteins. *Exp. Eye Res.* 34:239–255.

Andries, Chr., W. Guedens, J. Clauwaert, and H. Geerts. 1983. Photon and fluorescence correlation spectroscopy and light scattering of eye-lens proteins at moderate concentrations. *Biophys. J.* 43:345–354.

Augustein, R. C. 1981. Protein modification in cataract: possible oxidative mechanisms. *In* Mechanisms of Cataract Formation in the Human Lens. G. Duncan, editor. Academic Press, Inc., London. 72–115.

Bargeron, C. B. 1973. Analysis of intensity correlation spectra of mixtures of polystyrene latex spheres by least squares. *Appl. Phys. Lett.* 23:379–381.

Bargeron, C. B. 1974. Measurement of a continuous distribution of spherical particles by intensity correlation spectroscopy: Analysis by cumulants. *J. Chem. Phys.* 61:2134–2136.

Bauer, D. R. 1980. Effects of aggregation on the hydrodynamics of concentrated latexes. A study by quasi-electric light scattering *J. Phys. Chem.* 84:1592–1598.

Benedek, G. B. 1971. Theory of transparency of the eye. *Appl. Opt.* 10:459–473.

Bettelheim, F. A. 1975. On the optical anisotropy of lens fiber cells. *Exp. Eye Res.* 21:231–234.

Bettelheim, F. A. 1978. Induced optical anisotropy fluctuation in the lens of the eye. *J. Colloid Interface Sci.* 63:251–258.

Bettelheim, F. A., and A. A. Bettelheim. 1978. Small-angle light scattering studies on xylose cataract formation in bovine lenses. *Invest. Ophthalmol. Visual Sci.* 17:896–902.

Bettelheim, F. A., and M. Paunovic. 1979. Light-scattering of normal human lens. I. Application of random density and orientation fluctuation theory. *Biophys. J.* 26:85–99.

Bloemendal, H. 1982. Lens proteins. C.R.C. *Crit. Rev. Biochem.* 12:1–38.

Brown, J. C., P. N. Pusey, J. W. Goodwin, and R. H. Ottewill. 1975. Light scattering study of dynamic and time-averaged correlations in dispersions of charged particles. *J. Phys. A.* 8:664–682.

Chen, F. C., A. Yeh, and B. Chu. 1977. Dynamics of calf-thymus DNA by single clipped photon correlation. *J. Chem. Phys.* 66:1290–1305.

Clark, J. J., and G. B. Benedek. 1980. The effects of glycols, aldehydes and acrylamide on phase separation and opacification in the calflens. *Invest. Ophthalmol. Visual Sci.* 19:771–776.

Delaye, M., and A. Gromiec. 1983. Mutual diffusion of crystallin proteins at finite concentrations: a light-scattering study. *Biopolymers.* 22:1203–1221.

Delaye, M., and A. Tardieu. 1983. Short-range order of crystallin proteins accounts for eye lens transparency. *Nature (Lond.).* 302:415–417.

Delaye, M., J. J. Clark, and G. B. Benedek. 1982. Identification of the scattering elements responsible for lens opacification in cold cataracts. *Biophys. J.* 37:647–656.

Doty, P., and R. F. Steiner. 1952. Macro-ions I. Light-scattering theory and experiments with BSA. *J. Chem. Phys.* 20:85–94.

Giordano, R., G. Maisano, F. Mallamace, N. Micali, and F. Wanderlingh. 1981*a*. Structural properties of macromolecular solutions. *J. Chem. Phys.* 75:4770–4775.

Giordano, R., M. P. Fontana, and F. Wanderlingh. 1981*b*. Thixotropic behaviour of lysozyme solutions. *J. Chem. Phys.* 74:2011–2015.

Hamilton, W. C. 1965. Significance tests on the crystallographic R factor. *Acta Crystallogr.* 18:502–510.

Harding, J. J., and K. J. Dilley. 1976. Structural proteins of the mammalian lens: a review with emphasis on changes in development, aging and cataract. *Exp. Eye Res.* 22:1–73.

Jedziniak, J. A., D. F. Nicoli, H. Baram, and G. B. Benedek. 1978. Quantitative verification of the existence of high molecular weight protein aggregates in the intact normal human lens by light-scattering spectroscopy. *Invest. Ophthalmol. Visual Sci.* 17:51–57.

Jones, G., and D. Caroline. 1979. Intramolecular relaxation of polystyrene in a theta solvent by photon-correlation spectroscopy. *Chem. Phys.* 37:187–194.

Kerker, M. 1969. Scattering by liquids. *In* The Scatterng of Light and Other Electromagnetic Radiation. M. Kerker, editor. Academic Press, Inc., London. 487–573.

Koppel, D. E. 1972. Analysis of macromolecular polydispersity in intensity correlation spectroscopy: the method of cumulants. *J. Chem. Phys.* 57:4814–4820.

Laiken, S. L., and M. P. Printz. 1970. Kinetic class analysis of hydrogen-exchange data. *Biochemistry.* 9:1547–1553.

Lee, S. P., and P. Chu. 1974. Least-squares integration method in intensity fluctuation spectroscopy of macromolecular solutions with bimodal distributions. *Appl. Phys. Lett.* 24:261–263.

Marshall, A. G. 1978. Scattering phenomena. *In* Biophysical Chemistry: Principles, Techniques and Applications. A. G. Marshall, editor. John Wiley & Sons, Inc., New York. 463–506.

Mathiez, P., G. Weisbuch, and C. Mouttet. 1979. Inelastic light-scattering study of polyadenilic acid. *Biopolymers.* 18:1465–1478.

Mathiez, P., C. Mouttet, and G. Weisbuch. 1981. Quasi-elastic light-scattering study of polyadenylic acid solutions II. *Biopolymers.* 20:2381–2394.

Nieuwenhuis, E. A., C. Pathmanoharan, and A. Vrij. 1981. Liquid-like structures in concentrated latex dispersions. A light-scattering study of PMMA particles in benzene. *J. Colloid Interface Sci.* 81:196–213.

Nieuwenhuysen, P. 1978. Photon-count autocorrelation spectroscopy. Data analysis in the case of monoexponential spectra. *Macromolecules.* 11:832–833.

Ostrowsky, N., D. Sornette, P. Parker, and E. R. Pike. 1981. Exponential sampling method for light scattering polydispersity analysis. *Opt. Acta.* 28:1059–1070.

Patkowski, A., and B. Chu. 1979. Intensity fluctuation spectroscopy and transfer RNA conformation. III. Influence of NaCl concentration on the size and shape of the initially salt-free tRNA in solution. *Biopolymers.* 18:2051–2072.

Patkowski, A., E. Gulari, and B. Chu. 1980. Long-range tRNA-tRNA electrostatic interactions in salt free and low-salt tRNA solutions. *J. Chem. Phys.* 73:4178–4184.

Phillies, G. D. J. 1974. Effects of intermacromolecular interactions on diffusion. I. Two-component solutions. II. Three-component solutions. *J. Chem. Phys.* 60:976–983.

Pike, E. R., W. R. M. Pomorey, and J. M. Vaughan. 1975. Measurement of rayleigh ratio for several pure liquids using a laser and monitored photon counting. *J. Chem. Phys.* 62:3188–3192.

Pusey, P. N. 1978. Intensity fluctuation spectroscopy of charged Brownian particles: the coherent scattering function. *J. Phys. A Math. Gen.* 11:119–135.

Siezen, R. J., and J. H. Hoenders. 1979. The quaternary structure of bovine α-crystallin. Effects of variation in alkaline pH, ionic strength, temperature and calcium ion concentration. *Eur. J. Biochem.* 111:435–444.

Siezen, R. J., and E. A. Owen. 1983. Interactions of lens proteins. Self-association and mixed-associatoin studies of bovine α-crystallin and γ-crystallin. *Biophys. Chem.* 18:181–194.

Sørensen, C. M., R. C. Mockler, and W. J. O'Sullivan. 1976. Depolarized correlation function of light double scattered from a system of Brownian particles. *Phys. Rev. A.* 14:1520–1532.

Sørensen, C. M., R. C. Mockler, and W. J. O'Sullivan. 1978. Multiple scattering from a system of Brownian particles. *Phys. Rev. A.* 17:2030–2035.

Spector, A., L-K. Li, R. C. Augusteyn, A. Schneider, and T. Freund. 1971. The isolation and characterisaton of distinct macromolecular fractions. *Biochem. J.* 124:337–343.

Stauffer, J., C. Rothschild, Th. Wandel, and A. Spector. 1974. Transformation of alpha-crystallin polypeptide chains with aging. *Invest. Ophthalmol.* 13:135–146.

Tanaka, T., and G. B. Benedek. 1975. Observation of protein diffusivity in intact human and bovine lenses with applications to cataract. *Invest. Ophthalmol.* 13:135–146.

van Helden, A. K., and A. Vrij. 1980. Static light scattering of concentrated silica dispersions in apolar solvents. *J. Colloid Interface Sci.* 78:312–329.

Van Kamp, G. J., L. H. M. Schats, and H. J. Hoenders. 1973. Characterisation of α-crystallin related to fiber cell development in calf eye lenses. *Biochim. Biophys. Acta.* 295:166–173.